Bulletin of the Geological Survey of Japan, vol.57 (3/4), p. 73- 88 , 2006

Paleomagnetism of the Lower to Middle Miocene Series in the Yatsuo area, eastern part of southwest Japan: clockwise rotation and marine transgression during a short period

Machiko Tamaki[1,*], Yasuto Itoh[1] and Mahito Watanabe[2]

Machiko Tamaki, Yasuto Itoh and Mahito Watanabe (2006) Paleomagnetism of the Lower to Middle Miocene Series in the Yatsuo area, eastern part of southwest Japan: clockwise rotation and marine transgression during a short period. *Bull. Geol. Surv. Japan*, vol. 57 (3/4), 73-88, 8 figs, 1 table.

Abstract: Process of the tectonic rotation related to Japan Sea opening is viewed from tilt-corrected paleomagnetic data obtained from the Early to Middle Miocene sequence in the Yatsuo area on the Japan Sea coast, eastern part of southwest Japan. Progressive demagnetization experiments have been executed on samples obtained from two routes along the Yamada and Wada Rivers, and successfully isolated stable primary magnetic components in 16 sites. Together with data of previous studies, tilt-corrected reliable paleomagnetic directions comprising 10 normal and 27 reversed polarity sites of the Yatsuo Group on accurate stratigraphic positions show systematic temporal variation of easterly deflection in declinations. On the basis of our presented magnetostratigraphy, Yatsuo Group is assigned from the late Early to early Middle Miocene. Significant stage of rotation as much as 30° is specified during late Early Miocene between a period of active volcanism and subsequent period of marine transgression. We suggest that the Japan Sea opening event had a final phase of rapid rotation around the late Early Miocene, which seems to have caused marine transgression in relation to remarkable subsidence along the Japan Sea coast.

Keywords: back-arc opening, Japan Sea, clockwise rotation, subsidence, paleomagnetism, paleoenvironment, southwest Japan, Miocene

1. Introduction

Japan Sea is considered as a back-arc basin which was rifted through the late Cenozoic. Its origin has been investigated by many researchers mainly upon the basis of ODP offshore drilling and paleomagnetism of subaerial rocks. Paleomagnetic studies in 1980's (e.g. Otofuji and Matsuda, 1983; 1984; Otofuji *et al.*, 1985) suggested that southwest Japan suffered nearly 50° clockwise rotation at about 15 Ma, and that this event was caused by the back-arc opening. Their age estimate seems discordant with heat-flow data in the Japan Sea which imply older formation of the basin (>20 Ma; Tamaki, 1986). Such discrepancy of the event ages between the back-arc opening and rotation was once interpreted as two stages of the opening (Hayashida *et al.*, 1991): clockwise rotation of southwest Japan between 16 and 14 Ma associated with fan-shaped opening after drift of the Japanese islands before 16 Ma as a result of parallel opening. Although many kinematic models have been submitted to explain the nascent status of the island arc (e.g. Jolivet *et al.*, 1994), temporal succession of tectonic events have not been established. In order to understand mechanism of the Japan Sea opening and rotation during the short-lived events, sequential paleomagnetic data with precise age assignment should be collected in more detail.

Otofuji *et al.* (1985) discussed rotational process based on temporal change of magnetic declinations reported from wide-spread areas in southwest Japan. Later, Itoh (1988) suggested that the eastern part of southwest Japan had suffered differential rotation just after the coherent clockwise rotation related with the back-arc opening, and attributed the latter rotational event to an intra-arc deformation raised by a collision of the Izu-Bonin Arc (Fig. 1). Since differential rotation was also found on the western end of southwest Japan (Ishikawa, 1997), the rotational process should be reassessed on the basis of sequential declination data obtained from a confined area in which effects of local deformation can be eliminated referring to geological structure.

[1] Department of Physical Science, Graduate school of Science, Osaka Prefecture University, Gakuen-cho 1-1 Sakai, Osaka 599-8531, Japan.

[2] Geological Survey of Japan, AIST, Central 7, 1-1-1 Higashi, Tsukuba 305-8567, Japan.

* Correspondence.

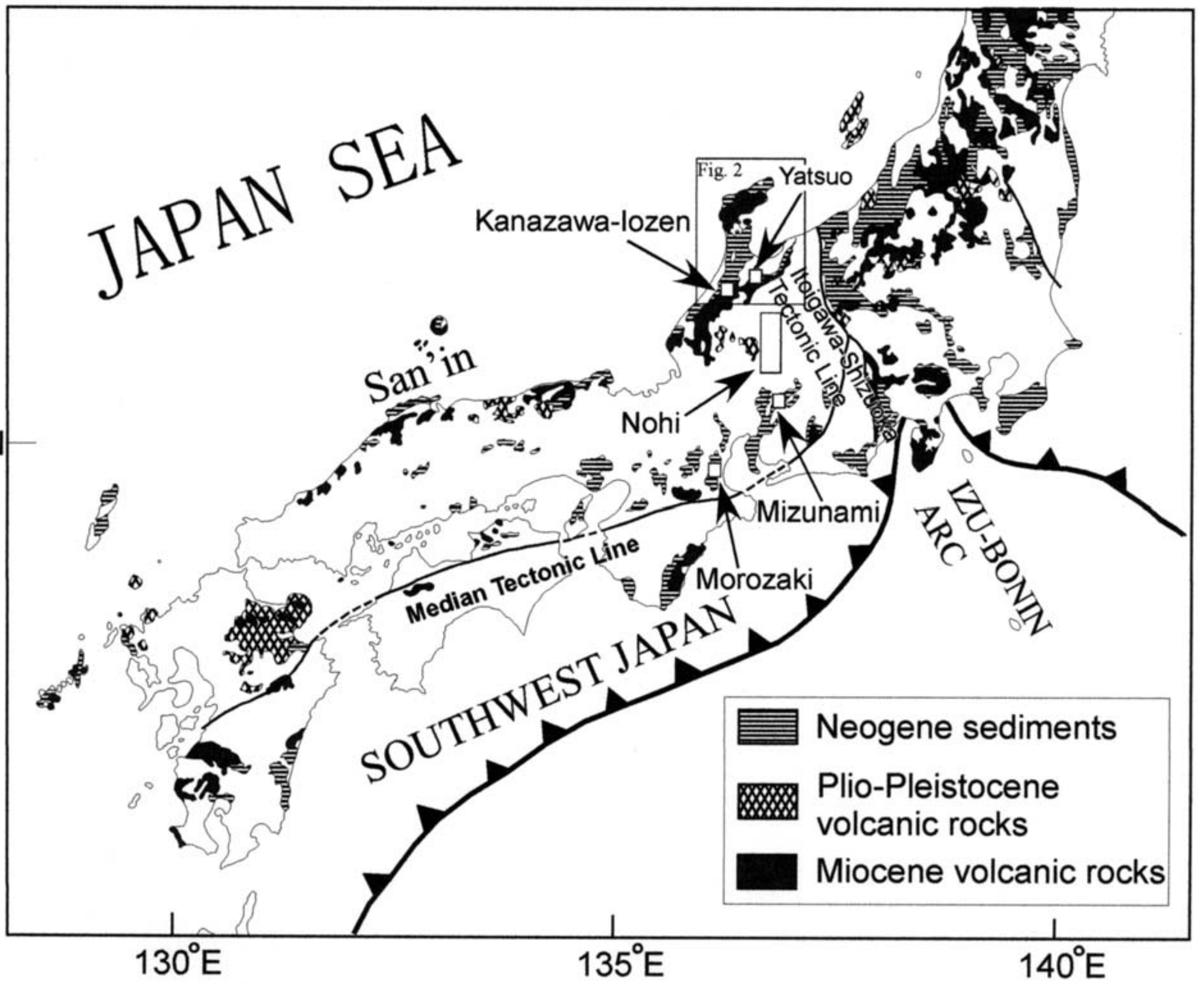

Fig. 1 Map showing the geological setting around southwest Japan. Enclosures show the survey areas of the present study and Itoh and Kitada (2003).

Previous studies of tectonic rotation related to Japan Sea opening were reported in the San'in, Mizunami, Morozaki, and Kanazawa-Iozen areas (Fig. 1). Otofuji *et al.* (1991) discussed timing of clockwise rotation of the San'in district in central part of southwest Japan, but their target samples were only from the volcaniclastic or volcanic rocks, for which tectonic tilting is generally difficult to be corrected. In order to discuss rotational process on the basis of sequential data-set, paleomagnetic samples should be collected where structural attitudes are obvious to determine accurate stratigraphic positions. Hayashida (1986) also reported clockwise rotation linked to Japan Sea opening based on sedimentary rocks in the Mizunami and Morozaki areas where sedimentary basins are representing intra-arc basins. For the purpose of more detailed description of the rotational process related to Japan Sea opening, paleomagnetic data should be obtained from marine transgressive sediments along the back-arc margin. Itoh and Kitada (2003) executed paleomagnetic study intended for tilt-corrected samples in the Kanazawa-Iozen area. However their rotational process was not conclusive for the following two reasons. One reason is that they discussed rotational process with the inconsistency between the magnetostratigraphy and the diatom biostratigraphy, which would decrease certainty of timing of tectonic rotation. The other is that whole rotational process was not observed in their area due to stagnant sedimentation (Yanagisawa, 1999a).

In the present study, we focus on the Yatsuo area on the Japan Sea coast (Fig. 1) where Lower to Middle Miocene Series composed of volcanic rocks and sedimentary rocks are well exposed without unconformity or structural disturbance. On the basis of the stratigraphic study (Hayakawa and Takemura, 1987), sedimentary facies of the strata in this area shows distinct trend of marine transgression. This study area is suited to submit a basic sequential paleomagnetic data-set recording rotational process during the marine transgression. Previous paleomagnetic studies have been conducted in our study area (e.g. Itoh and Hayakawa, 1988; 1989; Itoh and Watanabe, 2000). However, their presented data-set were small in number especially samples from volcanic rocks, so that it was difficult to constrain timing and magnitude of tectonic rotation with precise age assignment. In addition, their magnetostratigraphy was not concordant with biostratigraphy established by Yanagisawa (1999b). In order to solve such controversy, more integrated stratigraphic correlation based on sequential paleomagnetic data is still required in this study area. Hence, we aim to refine magnetostratigraphy and specify significant stage of rotation using difference among time-averaged formation-mean declinations. Spatial differences between the Yatsuo area and previous studied areas in the eastern part of the south-west Japan are also estimated to confirm deformation mode proposed by Itoh (1988) and Itoh and Ito (1989). Finally, tectonic implications of the paleoenvironmental changes around the rapid rotation are described on the basis of stratigraphic order of back-arc opening events.

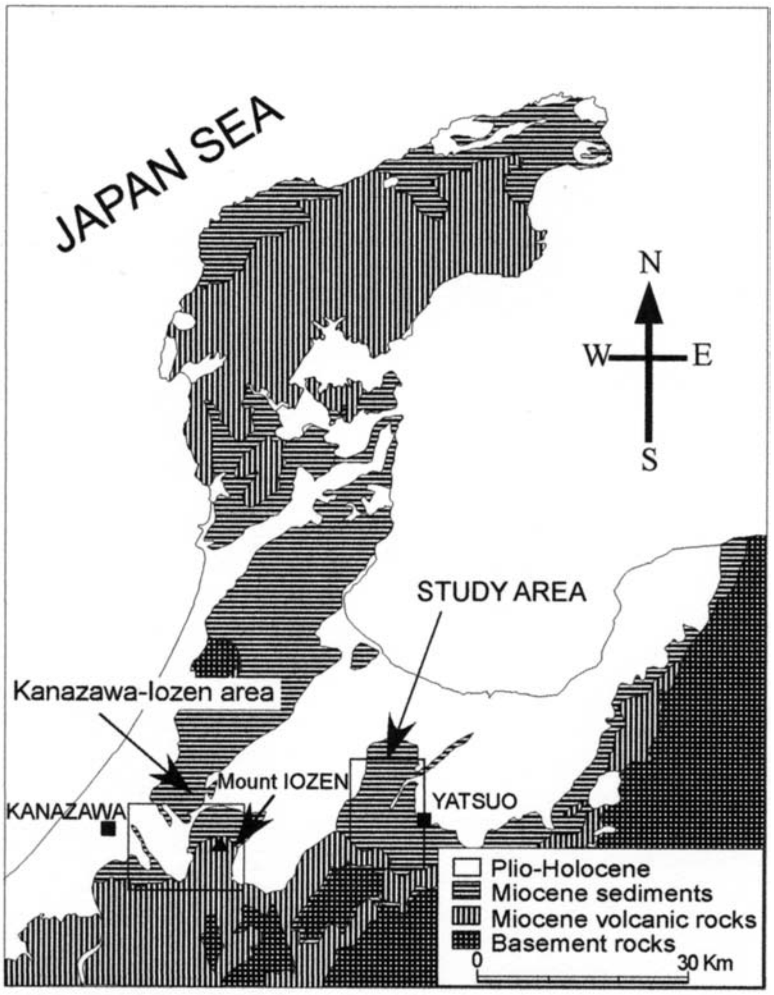

Fig. 2 A geological map in the Hokuriku district upon the Japan Sea coast of the eastern part of southwest Japan.

2. Geological setting and sampling

Yatsuo area is underlain by Neogene volcanic and marine sedimentary rocks (Fig. 2). This Neogene System is divided into two groups; the lower Yatsuo and the upper Tonami Groups (Hayakawa and Takemura, 1987). The Yatsuo Group, schematically shown in Fig. 3, is about 3,000 m thick, and divided into five formations: Nirehara, Iwaine, Iozen, Kurosedani and Higashibessho, in ascending order. The Nirehara Formation is mainly composed of conglomerates and sandstones. The Iwaine and Iozen Formations consist of andesitic and rhyolitic volcanic/volcaniclastic rocks, respectively. The Kurosedani Formation is composed of sandstone and siltstone, which shows an upward-fining sequence. The Higashibessho Formation is rich in siltstone. Diatom biostratigraphy of the Early to Middle Miocene sedimentary units (Higashibessho Formation) was established by Yanagisawa (1999b) (Fig. 3c). The correlation between a standard geomagnetic polarity timescale (Fig. 3a) and diatom biohorizons are based on Watanabe and Yanagisawa (2005) (Fig. 3b).

Samples for the paleomagnetic analysis were collected at 26 sites from the Yatsuo Group by using an engine drill or an electric drill. Eight to 15 cores 25 mm in diameter were drilled from each site and the individual cores were oriented with a Brunton compass mounted on an aluminum orientation table. Reported paleomagnetic directions in the Yatsuo area (Itoh and Hayakawa, 1988; 1989; Itoh and Watanabe, 2000) were particularly scarce in the Iwaine and Iozen Formations. As for the lower volcanic units, which have been intensively sampled in the present study, a lithologic columnar section and sampling horizons are shown in Fig. 3. We selected two sampling routes along the Yamada River and the Wada River (Fig. 4). Columnar sections of these routes are combined using a key bed, Yamadanaka tuff (Figs. 3, 4) which intercalates the upper part of the Yamada River section, and lower part of the Wada River section. In both routes, the strata gently dip northward without serious tectonic disturbance. In the Yamada River route, the Iwaine and Iozen Formations include initially horizontal water-laid bedded tuff layers (Fig. 3) showing the same structural attitude as the overlying sedimentary units, which intercalate with volcanic and volcaniclastic rocks. Along the routes, we selected sampling sites where we can define bedding attitude for tilt correction of paleomag-

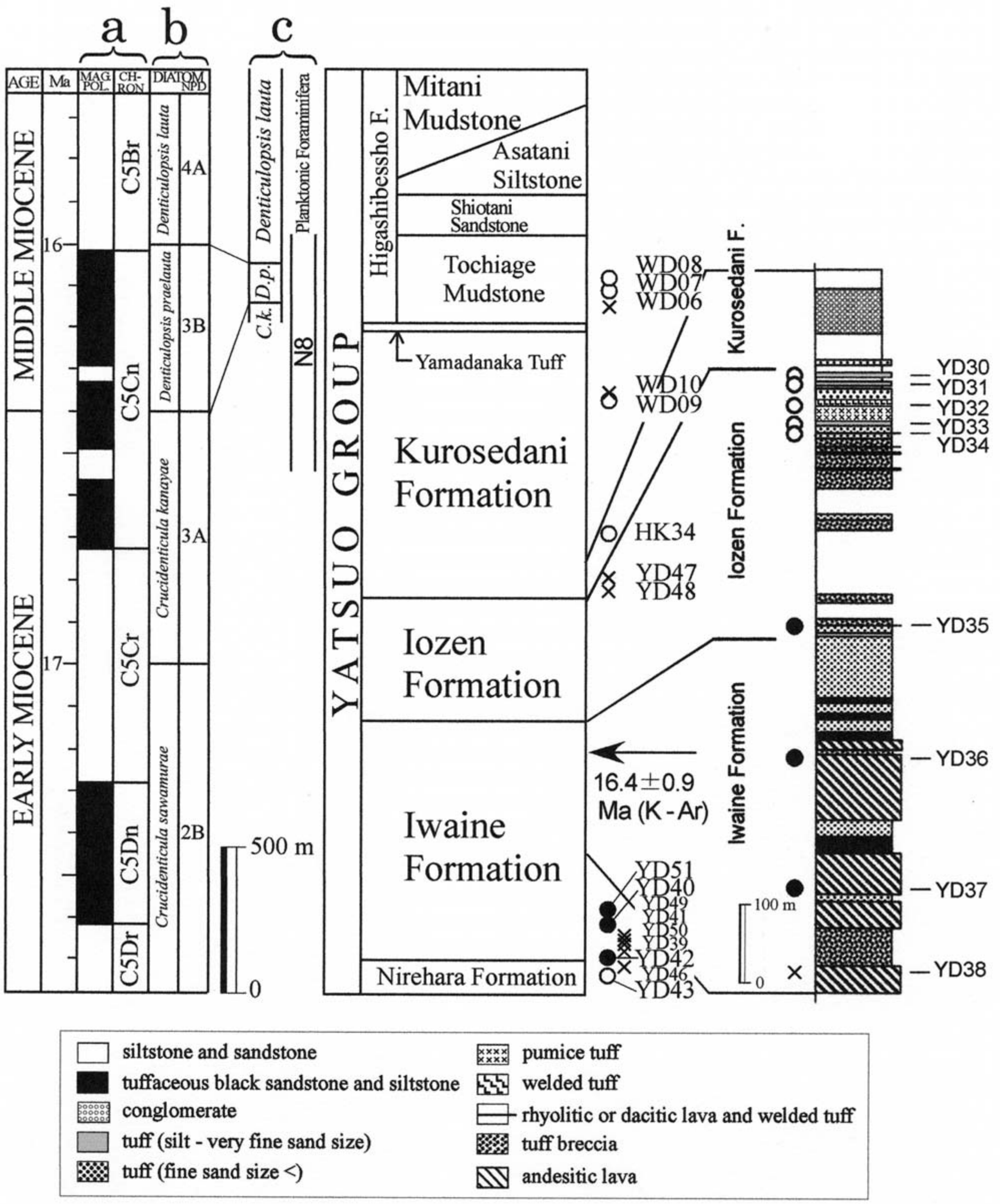

Fig. 3 Geological units after Hayakawa and Takemura (1987) and stratigraphic horizons of paleomagnetic samples of this study. Solid (open) symbols correspond to normal (reversed) polarity data. Christ cross shows primary component is not obtained. As for the lower volcanic units, which have been intensively sampled in the present study, lithologic columnar section and sampling horizons are attached on the right. Chronological information is summarized as: a) Standard geomagnetic time-scale (Cande and Kent, 1995), b) Diatom biohorizons based on ODP Leg 145 site 887C (Watanabe and Yanagisawa, 2005), c) Diatom biostratigraphy and planktonic foraminifera biostratigraphy of sedimentary units in the Yatsuo area (Yanagisawa, 1999b).

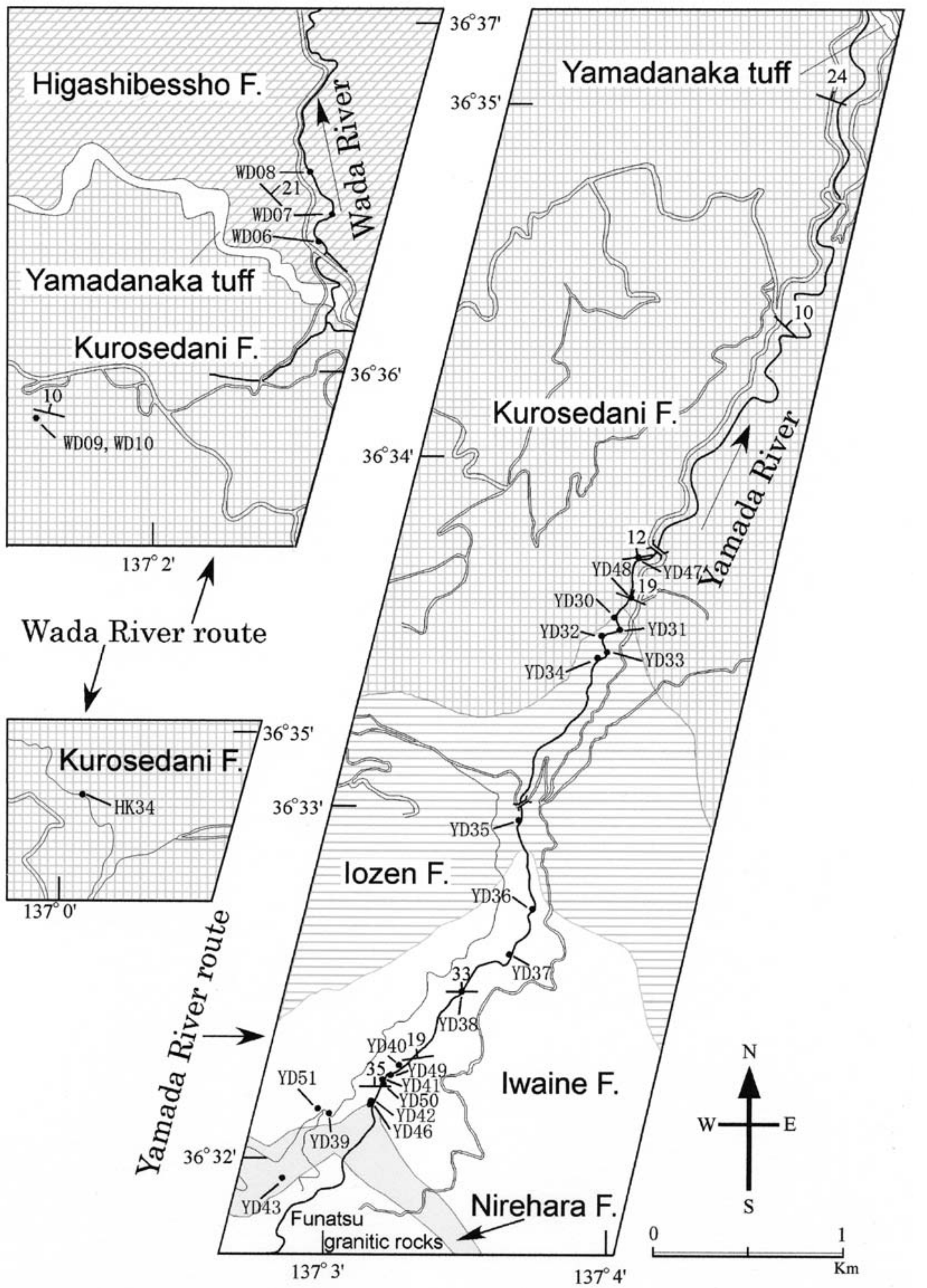

Fig. 4 Paleomagnetic sampling localities along the Yamada River and Wada River routes with simplified geologic information after Hayakawa and Takemura (1987) and Nozawa and Sakamoto (1960).

netic directions. Rock types and strike-dip data used for tilt correction of each site are listed in Table 1.

3. Paleomagnetism

In the laboratory, the samples were cut into cylindrical specimens of 25 mm in diameter and 22 mm in length. Each sampling site contained eight to 26 standard-sized specimens. Remanent magnetization was measured for all specimens by using a spinner magnetometer (Natsuhara Giken SSM-1A) or a cryogenic magnetometer (2-G Enterprise model 760). In order

Table 1 Site mean magnetic directions from the Yatsuo Group

Site	Facies	Latitude	Longitude	Strike	Dip	Method	DMG	D	I	Dc	Ic	α_{95}	k	N	ϕ	λ	Ref.
Higasibessho Formation																	
Mitani Mudstone																	
HR40	mudstone							-45.4	65.4	-19.4	43.3	6.8	78.8	7	69.9	18.0	2
Asatani Siltstone																	
YT11	siltstone							130.8	-75.9	170.4	-53.1	19.5	9.0	8	81.6	29.3	2
HR11	silty tuff							142.2	-73.7	177.2	-60.6	7.9	43.6	9	84.6	-114.3	2
HR43	siltstone							151.2	-69.9	175.6	-54.1	9.7	33.5	8	85.9	19.4	2
Shiotani Sandstone																	
05	tuff							-143.5	-84.9	-172.5	-51.7	3.2	190.1	12	82.5	-100.5	2
YT04	tuff							-36.9	-63.0	-164.9	-73.1	5.9	68.9	10	65.8	156.3	2
Tochiage Mudstone																	
WD08	mudstone	36.6095	137.0423	N 44° W	21° E	PCA	PAFD	-166.7	-60.6	-154.8	-41.7	7.3	50.4	9	(65.0)*	(-109.8)*	1
WD07	mudstone	36.6075	137.0436	N 44° W	21° E	PCA	PAFD	167.9	-65.1	-167.9	-50.1	7.8	74.6	6	(78.4)*	(-106.8)*	1
WD06	mudstone	36.6061	137.0428	N 40° W	23° E												1
YT28	mudstone							-179.3	-53.6	-163.4	-34.2	9.5	30.1	9	67.0	-86.7	2
Kurosedani Formation																	
33	tuff							171.6	-52.3	-174.0	-45.7	4.9	80.1	12	79.3	-72.9	2
YD16	siltstone							148.4	-64.1	-177.8	-51.4	6.6	103.8	6	85.1	-65.4	4
WD10	mudstone	36.5978	137.0264	N 83° W	10° N												1
WD09	tuff	36.5978	137.0264	N 83° W	10° N	PCA	PThD	134.2	-59.0	145.0	-52.2	7.5	65.2	7	(61.1)*	(49.9)*	1
YD20	siltstone							-177.7	-53.0	-160.9	-45.7	5.9	106.9	7	71.3	-108.1	4
YD21	siltstone							163.0	-51.3	178.3	-48.7	5.2	97.3	9	82.9	-30.8	4
YD22	siltstone							163.2	-34.6	171.2	-29.1	8.2	55.8	7	67.6	-20.2	4
YD23	siltstone							176.9	-50.9	-175.9	-43.4	10.1	45.0	6	78.2	-61.4	4
YD25	siltstone							-169.0	-72.4	-174.4	-49.6	7.3	69.4	7	82.3	-81.8	4
YD44	siltstone							52.3	34.3	47.5	35.7	7.5	56.0	8	45.4	-124.1	5
YD45	siltstone							28.5	43.7	22.1	42.1	10.2	26.6	9	67.4	-106.2	5
HK34	tuff	36.5803	137.0013	N 34° W	35° N	PCA	PThD	-174.7	-84.5	-130.8	-51.3	2.0	799.7	8	(49.5)*	(-141.4)*	1
HR49	very fine sandstone							179.5	-61.8	-174.8	-47.3	13.1	22.3	7	80.8	-72.8	3
YD47	very fine sandstone	36.5618	137.0683	N 82° E	12° N	PCA	PAFD	4.6	49.0	(YD47-53)							1
YD48	very fine sandstone	36.5612	137.0679	N 58° W	19° N	PCA	PThD	-1.6	52.4	(YD48-32)							1
Iozen Formation																	
YD30	tuff	36.5591	137.0668	N 82° W	16° N	PCA	PThD	-118.5	-41.2	-127.3	-30.7	8.8	59.1	6	(39.5)*	(-124.2)*	1
YD31	tuff	36.5584	137.0674	N 72° W	14° N	PCA	PThD	174.0	-78.4	-173.0	-65.0	11.0	26.4	8	(78.3)*	(161.4)*	1
YD32	tuff	36.5580	137.0662	N 72° W	14° N	PCA	PThD	-98.9	-58.0	-114.8	-49.9	6.4	88.6	7	(36.4)*	(-147.0)*	1
YD33	tuff	36.5573	137.0667	N 89° E	13° N	PCA	PThD	-127.5	-46.1	-136.0	-37.2	13.0	22.5	7	(48.7)*	(-122.8)*	1
YD34	lava	36.5571	137.0659	N 86° W	19° N	PCA	PThD	-148.3	-31.3	-151.8	-14.2	8.1	47.5	8	(51.0)*	(-91.1)*	1
HR46	tuff							-155.3	-63.6	-152.2	-53.8	9.9	38.4	7	67.3	-135.6	3
YD35	welded tuff	36.5492	137.0613	N 83° W	24° N	PCA	PAFD	59.9	61.9	38.2	43.7	2.2	556.8	9	(55.7)*	(-125.2)*	1
36	welded tuff							42.7	58.2	18.3	48.7	2.0	790.8	8	73.2	-113.9	2

Table 1 (continued)

Site	Facies	Latitude	Longitude	Strike	Dip	Method	DMG	D	I	Dc	Ic	α_{95}	k	N	ϕ	λ	Ref.
Iwaine Formation																	
HK58	andesite							42.6	55.8	26.5	41.3	3.3	176.4	12	63.9	-110.9	2
YD36	andesite	36.5452	137.0622	N 80° E	33° N	PCA	PAFD	84.7	72.7	20.6	54.5	6.0	74.7	9	(73.3)*	(-133.9)*	1
YD37	andesite	36.5428	137.0608	N 63° W	37° N	PCA	PThD	76.3	53.1	56.8	23.8	6.7	68.5	8	(33.9)*	(-122.9)*	1
YD38	andesite	36.5412	137.0580	N 89° E	33° N												1
35	andesite							70.3	61.4	17.9	41.7	4.3	143.1	9	70.2	-98.8	2
YD51	andesite	36.5357	137.0498	N 88° W	24° N	PCA	PThD	128.2	48.2	98.0	57.3	6.1	25.8	23	(16.1)*	(-168.5)*	1
YD40	andesite	36.5380	137.0546	N 86° E	19° N	PCA	PAFD	103.9	55.0	75.6	56.3	2.8	343.7	9	(31.1)*	(-158.1)*	1
YD49	tuff	36.5371	137.0540	N 82° E	44° N												1
YD41	tuff	36.5370	137.0531	EW	35° N												1
YD50	andesite	36.5366	137.0535	N 82° E	18° N												1
YD39	andesite	36.5352	137.0504	N 27° E	19° E												1
YD42	andesite	36.5360	137.0523	N 16° E	50° W	PCA	PThD	66.9	45.9	-8.8	61.1	5.2	114.8	8	(81.2)*	(89.4)*	1
YD46	tuff	36.5354	137.0522	N 17° E	55° W												1
Nirehara Formation																	
YD43	siltstone	36.5323	137.0480	N 80° E	30° N	RC	PAFD	-154.3	-52.2	-166.6	-25.8	7.5	75.3	8	(64.1)*	(-74.0)*	1
HK53	silty tuff							-70.1	-73.6	-166.8	-60.6	4.8	114.2	9	78.6	-163.1	2
HK50	siltstone							-140.6	-72.9	-160.1	-49.8	2.7	262.9	12	72.4	-119.0	2

Latitude and Longitude, International Terrestrial Reference Frame (ITRF); Strike and Dip, the strike-dip data used for tilt corrections; RC and PCA, the remagnetization circle analysis (McFadden and McElhinny, 1988) and principal component analysis (Kirschvink, 1980), respectively; PAFD and PThD, progressive alternating field demagnetization and progressive thermal demagnetization, respectively; D and I, in situ site-mean declination and inclination before tilt corretion in degrees, respectively; Dc and Ic, site-mean declination and inclination after tilt correction in degrees, respectively; α_{95}, radius of 95% confidence circle in degrees; k, pression parameter; N, number of specimens; ϕ and λ, latitude and longitude of virtual geomagnetic pole for untilted site-mean direction, respectively.

*Data are calculated by ITRF.

Reference: 1, this study; 2, Itoh and Hayakawa (1988); 3, Itoh and Hayakawa (1989); 4, Itoh and Watanabe (2000); 5, Itoh and Watanabe (2006).

to isolate stable remanent magnetization components, progressive alternating field demagnetization (PAFD) and progressive thermal demagnetization (PThD) tests were carried out.

Two pilot specimens per one site which have average direction in natural remanent magnetization (NRM) were subjected to PAFD and PThD, respectively. Then we executed demagnetization of the rest of the specimens by PAFD or PThD methods, selecting more effective method to isolate a stable magnetic component. Results of the progressive demagnetization were analyzed using vector end-point orthogonal diagrams. Fig. 5 shows typical results of progressive demagnetization tests.

We identified single stable component in some sites, which are observed as straight trends converging to the origin of the diagrams (YD40-11, WD09-71; Fig. 5a, c). Such components show quite different directions from the present geomagnetic field. In other sites, two components were isolated (YD35-12; Fig. 5b); one low-temperature component (25 ℃ < unblocking temperature (T_{UB}) < 140 ℃) is parallel to the present geomagnetic field in *in situ* coordinates. We regard it as secondary magnetization acquired during the recent geologic period. The other high-temperature component (180 ℃ < T_{UB} < 640 ℃) converged to the origin of the diagrams without directional change after demagnetization above the Curie temperature of magnetite (580 ℃).

In order to identify carriers of the magnetic components in samples, we made stepwise acquisition experiment of isothermal remanent magnetization (IRM) on AF-demagnetized samples in direct magnetic fields up to 2 T (Fig. 6a). In most cases, the IRM intensity almost saturated in applied field around 0.2 T, whereas a sample from site YD35 did not show saturation up to 0.2 T. We interpret that the dominant carrier of the stable remanent magnetization in majority sites is magnetite, while site YD35 contains both magnetite and hematite. We then executed PThD of composite IRM. Using the method of Lowrie (1990), composite IRMs were imparted by applying direct magnetic fields 2.0, 0.4, 0.12 T imposed to the samples in three orthogonal directions. Fig. 6b-e presents typical decay curves of the three IRM components through stepwise thermal demagnetization up to 680 ℃. Results of sites YD43, YD40 and WD09 (Fig. 6b-d) indicate that the dominant magnetic phase is of soft coercivity fraction (< 0.12 T) with a broad distribution of T_{UB} below 580 ℃, and that the medium (0.12 - 0.4 T) and high (0.4 - 2 T) coercivity fractions are minor contribution. We interpret that these samples are dominated by magnetite. As for the site (YD35) (Fig. 6e), the dominant magnetic phase has soft coercivity with a broad distribution of T_{UB} below 640 ℃. All coercivity fractions are significantly reduced between 100 and 180 ℃, suggesting that the low T_{UB} component is carried by goethite. The high T_{UB} component demagnetized up to 640 ℃ is probably carried by magnetite and hematite with coarse grain size.

We interpreted the stable high T_{UB} components as primary magnetization and determined their directions using a three-dimensional least squares analysis technique (Kirschvink, 1980). For the samples with overlapped T_{UB} spectra (YD43; Fig. 5f), we adopted remagnetization circle method (McFadden and McElhinny, 1988); we regard cross point of remagnetization circles figured out from all specimens in one site as primary component. If a primary remanent magnetic vector was not obtained as a result of complete remagnetization (YD47; Fig. 5d) or quite erratic behavior during demagnetization tests (WD06; Fig. 5e), we excluded the site from further discussion. Finally mean directions were determined at 16 sites as listed in Table 1.

4. Discussion

4.1 Temporal variation in declinations and magnetostratigraphy

In the Yatsuo area, sequential sampling enabled us to assign paleomagnetic data to accurate stratigraphic positions. The variation in declinations as a function of the stratigraphic position (cumulative thickness) is shown in Fig. 7. It is noteworthy that the lower part of the sequence shows significant easterly declinations, while no significant deflection is observed in the upper part. This systematic temporal change in untilted declinations suggests coherent clockwise rotation of the Yatsuo area around a vertical axis, because both of the data with normal and reversed polarities show similar trend.

Previous magnetostratigraphy of the Yatsuo area (Itoh and Watanabe, 2000) was constrained by standard geomagnetic polarity time-scale (Berggren *et al.*, 1995) and a K-Ar age (Shibata, 1973). However, their interpretation was not coincident with biostratigraphy assigned to Barron and Gladenkov's (1995) diatom biochronology (Yanagisawa, 1999b). This is possibly because of undiscovered polarity transition interval(s) in the study section, and/or insufficient correlation of magnetostratigraphy and biostratigraphy established by Barron and Gladenkov (1995) based on the result of ODP Site 884B and 887. Recently, Itoh and Watanabe (2006) reported normal polarity interval in the Kurosedani Formation. Watanabe and Yanagisawa (2005) presented refined Early to Middle Miocene diatom biochronology for the middle- to high-latitude North Pacific based on the result of ODP Site 887C. Then, our paleomagnetic result can be correlated to a standard geomagnetic polarity time-scale (Cande and Kent, 1995) using the biostratigraphic data and the ra-

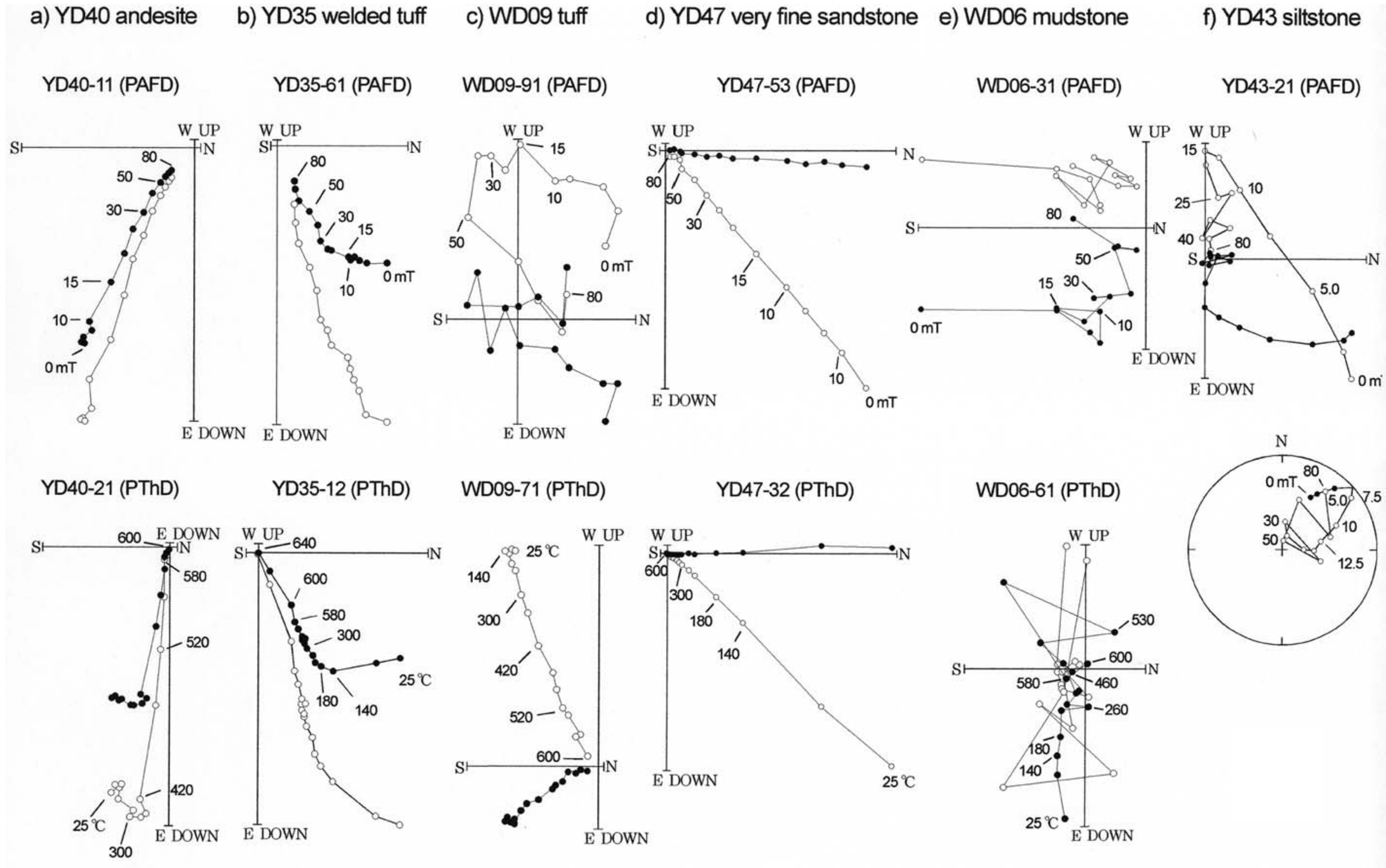

Fig. 5 Typical results of progressive alternating field demagnetization (PAFD) and progressive thermal demagnetization (PThD) before tilt correction. On the vector-demagnetization diagrams, solid (open) circles are projection of vector end-points on horizontal (N-S vertical) plane. As for the equal-area projections, solid (open) circles are on the lower (upper) hemisphere. Numbers attached on circles are demagnetization levels in ℃ or mT.

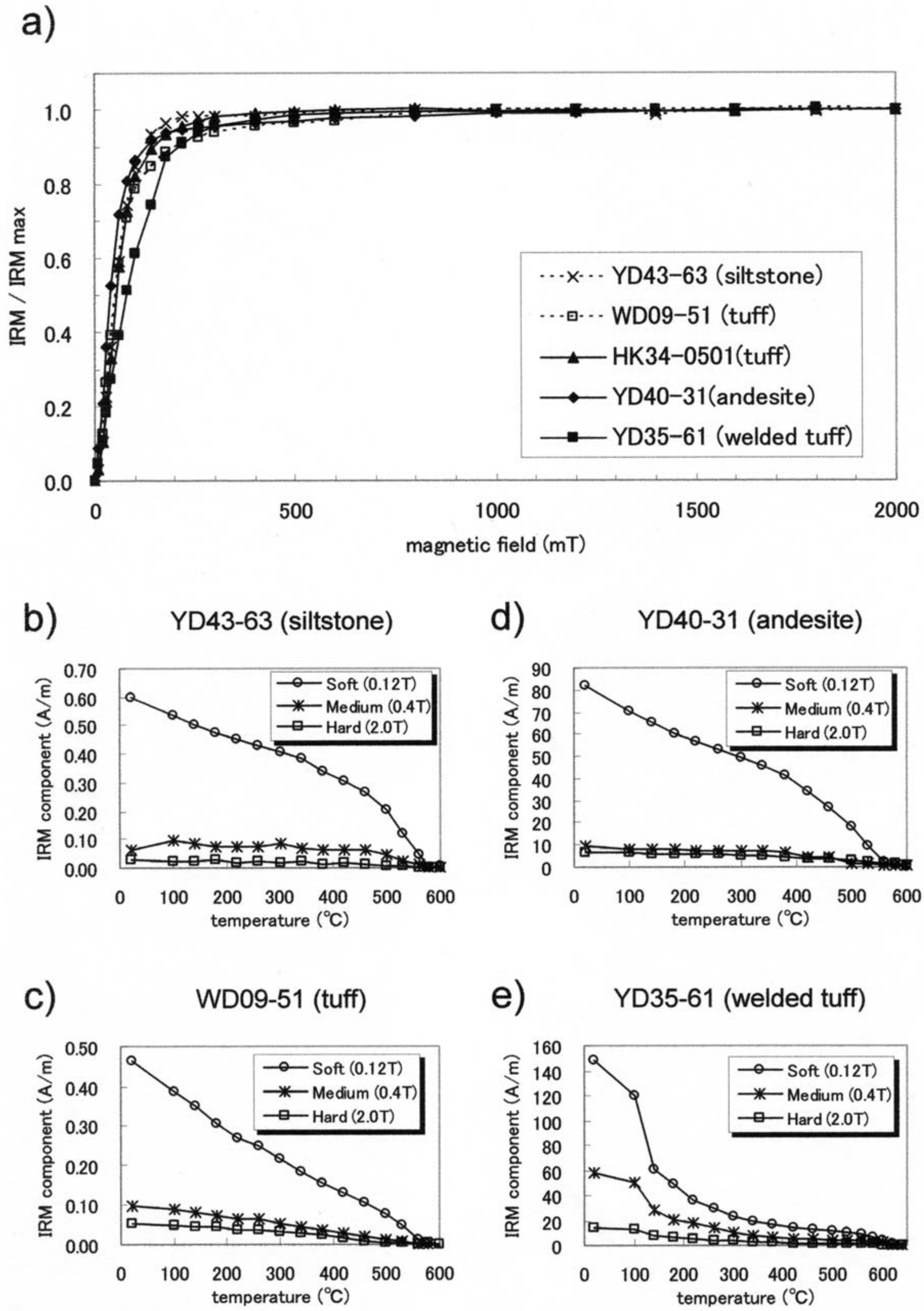

Fig. 6 a) Progressive acquisition of isothermal remanent magnetization (IRM) for volcanic and sedimentary rocks in the Yatsuo Group. b), c), d) and e) Thermal demagnetization curves of orthogonal IRM for samples from various rock types.

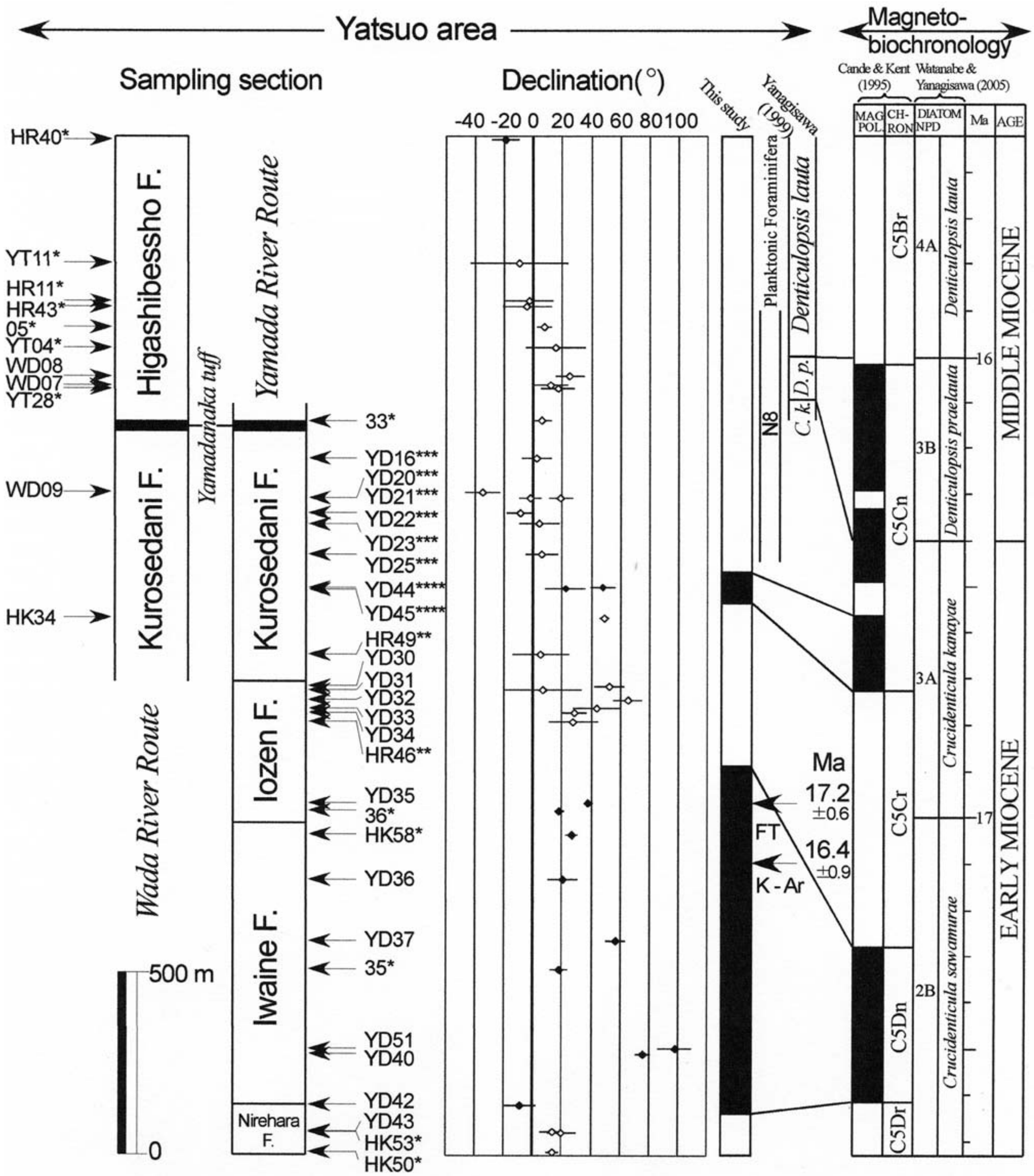

Fig. 7 Change of declinations versus thickness in the Yatsuo Group. Solid (open) symbols represent normal (reversed) polarity sites. Error bars show uncertainty in declination defined as $\sin^{-1}$ [$\sin \alpha_{95}$ /$\cos$ I] (α_{95}, radius of 95% confidence circle; I, inclination). Diatom biostratigraphy and planktonic foraminifera biostratigraphy are after Yanagisawa (1999b). K-Ar and fission-track ages were reported by Shibata (1973) and Itoh and Watanabe (2006), respectively. Standard geomagnetic time-scale and diatom biohorizons are based on Cande and Kent (1995) and Watanabe and Yanagisawa (2005), respectively. *Data from Itoh and Hayakawa (1988). **Data from Itoh and Hayakawa (1989). ***Data from Itoh and Watanabe (2000). ****Data from Itoh and Watanabe (2006).

diometric ages obtained from the studied formations. Yanagisawa (1999b) assigned the Higashibessho Formation to the *Crucidenticula kanayae* Zone (NPD 3A), the *Denticulopsis praelauta* Zone (NPD 3B) and *Denticulopsis lauta* Zone (NPD 4A) (Fig. 7). On the basis of biochronology (Watanabe and Yanagisawa, 2005), reversed polarity intervals correlated to these diatom zones are assigned to Chron C5Cn.2r, C5Cn.1r and C5Br, respectively because only reversed polarity data are obtained. Reversed polarity interval in the upper part of the Kurosedani Formation and normal polarity interval in the lower part of the Kurosedani Formation correspond to Chron C5Cn.2r and Chron C5Cn.3n, respectively. Reversed polarity interval in the upper part of the Iozen Formation and the lower part of the Kurosedani Formation is correlated to Chron C5Cr. Normal polarity interval in the Iwaine Formation and the lower part of the Iozen Formation is correlated to C5Dn. Radiometric ages obtained from the Iwaine Formation (16.4 ± 0.9 Ma; Shibata, 1973) and the Iozen Formation (17.2 ± 0.6 Ma; Itoh and Watanabe, 2006) are concordant with this correlation within the limits of error. Therefore the present result suggests that the Yatsuo Group is assigned from the late Early to early Middle Miocene. The C5Cn/C5Br chron boundary, which was correlated to the Iozen Formation by Itoh and Watanabe (1999), is located the lower part of the Higashibessho Formation based on revised correlation in this study. It is also necessary to modify magnetostratigraphy in the Kanazawa-Iozen area (Fig. 2), adjacent to the Yatsuo area. Although reversed polarity interval in the Sunagozaka/Nanamagari Formations was correlated to Chron C5Br (Itoh and Kitada, 2003), the *Crucidenticula Kanayae* Zone identified in the Sunagozaka/Nanamagari Formation (Yanagisawa, 1999a) is discordant to Chron C5Br on the basis of biochronology (Watanabe and Yanagisawa, 2005) (Fig. 7). Reversed polarity interval in the Sunagozaka/Nanamagari Formation should be correlated to C5Cn.2r and/or C5Cr using biostratigraphic data. However, this correlation is not concordant with the fission-track ages (15.0-15.4 Ma; Itoh *et al.*, 2000) in the Iozen Formation overlain by the Sunagozaka/Nanamagari Formation. Thus stratigraphic correlation between the Yatsuo and Kanazawa-Iozen areas remains further investigation.

4.2 Rotation during a short interval around the late Early Miocene

In this study, additional data to the Iwaine and Iozen Formations, from which few paleomagnetic data have been reported, allow us to submit time-averaged directions of the volcanic formations (Fig. 7). As shown in Fig. 8, mean directions of the Iozen and Higashibessho Formations represent antipodal normal and reversed polarities, indicating that the formation-means are calculated for enough time intervals. The Kurosedani Formation is a thick pile of sedimentary rocks (about 1,000 m thick), and paleomagnetic data were acquired from various rock types. Sampled interval of the Iwaine Formation is composed of several andesitic lava flows intercalated by tuff breccia layers. We regard that these formations also cover enough time intervals to average out the short-term fluctuations of geomagnetic field. Hence, each formation-mean provides a time-averaged paleomagnetic direction, which enables us to discuss tectonic rotation. In the Nirehara Formation, however, paleomagnetic data still remain fewer numbers than those of other formations, and sedimentary environments and depositional age are not known. Because influence of secular variation may not be negligible, we interpret that paleomagnetic data in the Nirehara Formation are difficult to compare with those of other formations, and exclude them from further discussion of formation-means.

Comparing amount of rotation (R) and its uncertainty (δR) calculated from the difference of formation-mean declinations in the Yatsuo Group, significant rotation as much as 30° (R=26.9°, δR=23.8°; δR is $[\delta D_1 + \delta D_2]^{1/2}$ [Beck, 1980]) is observed during the deposition of the Iozen and Kurosedani Formations (Fig. 8). On the basis of the age-estimation stated before (Fig. 7), it is suggested that most of rotation in this study area had been attained during a short interval around the late Early Miocene. The present result has specified a significant stage of rotation based on reliable paleomagnetic data with precise age assignment in the Yatsuo area for the first time.

Itoh and Ito (1989) suggested differential rotation within the Hokuriku district (Fig. 2) associated with ductile deformation in Japan arc. Later, Itoh and Kitada (2003) discussed more detailed rotational process in the Kanazawa-Iozen area (Fig. 2). In order to examine diachronous motion within the Hokuriku district, we calculate spatial difference of formation-mean declinations between the Yatsuo area and the Kanazawa-Iozen area. On the basis of the biostratigraphy (Yanagisawa, 1999a, b), the Sunagozaka/Nanamagari Formation in the Kanazawa-Iozen area which is assigned to the *Crucidenticula kanayae* Zone can be correlated to the Higashibessho Formation in the Yatsuo area. It is also possible that the Sunagozaka/Nanamagari Formation is assigned to the Kurosedani Formation because diatom zone in the Sunagozaka/Nanamagari Formation is recognized in the only upper part of the Nanamagari Formation (Yanagisawa, 1999a). Comparing formation-mean declinations in the Sunagozaka/Nanamagari Formation with the Kurosedani and Higashibessho Formations respectively, no significant difference is obtained (R=13.6°, δR=22.5° and R=18.9°, δR=23.6°; Fig. 8), suggesting that diachronous motion is not existence. This interpreta-

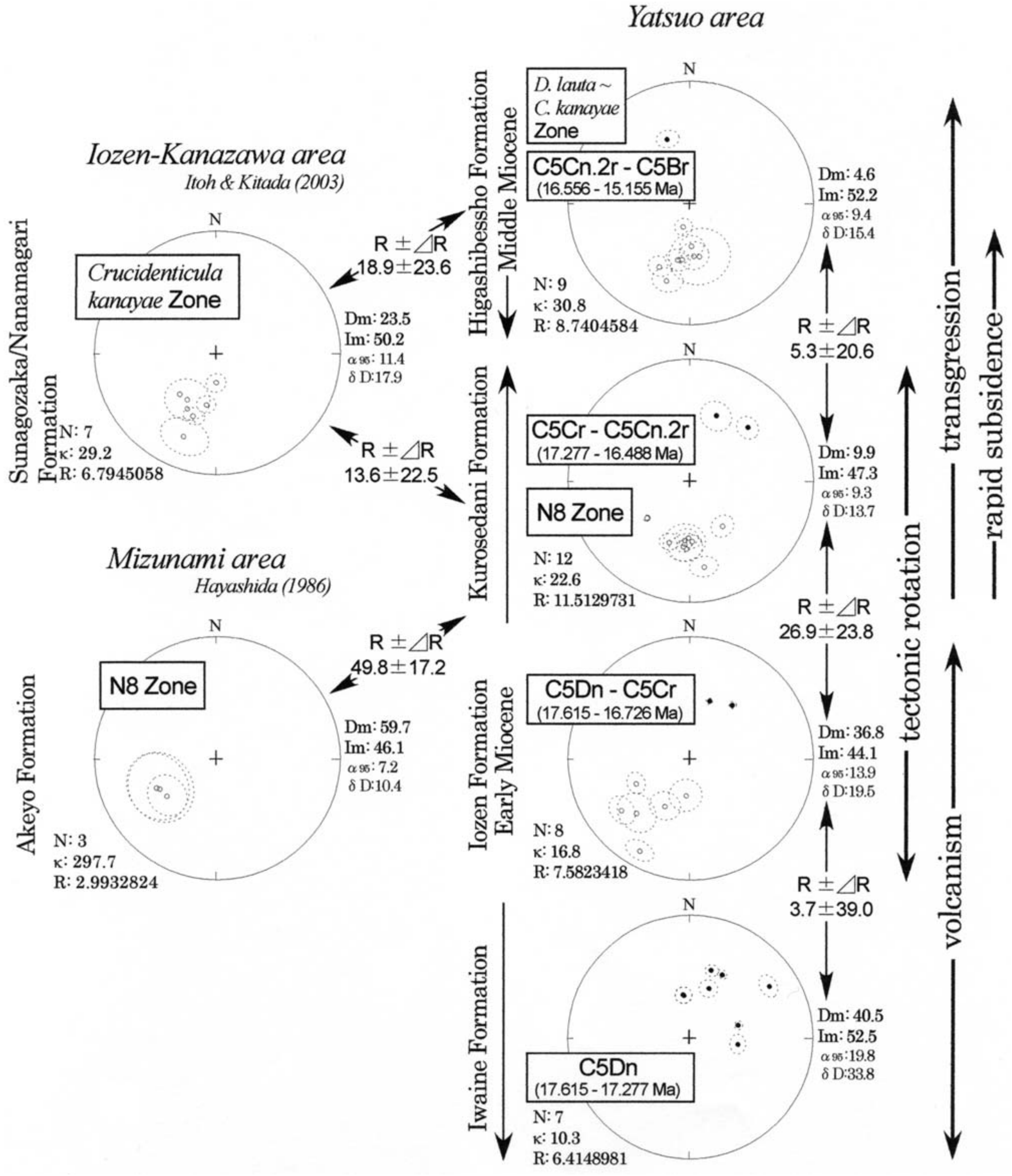

Fig. 8 Tilt-corrected site-mean magnetic directions divided into each formation in the Yatsuo, Kanazawa-Iozen (Itoh and Kitada, 2003) and Mizunami (Hayashida, 1986) areas. Solid (open) symbols are on the lower (upper) hemisphere of the equal-area projections. Dotted ovals are 95% confidence limits. Biostratigraphic data in the Kanazawa-Iozen and Yatsuo areas are after Yanagisawa (1999a, b). Chron ages for polarity reversal datums are from Cande and Kent (1995). R and ∂R ($[\partial D_1+\partial D_2]^{1/2}$) were defined by Beck (1980).

tion, however, is not conclusive and needs further investigations for two following reasons. One reason is that more integrated stratigraphic correlation between both areas is still required as stated above. The other is that detailed correlation of formation-mean data in the Sunagozaka/Nanamagari Formation reported by Itoh and Kitada (2003) to the presented data in the Yatsuo area is difficult because their formation-mean data were obtained from limited horizons of only tuff layers.

Itoh (1988) also proposed that the eastern part of south-west Japan had suffered differential rotation. However, their data-set of the Yatsuo area were summed up as Early Miocene data, and it is necessary to review spatial difference on the basis of paleomagnetic data with more precise age assignment. Comparing formation-mean directions between the Kurosedani Formation and the Akeyo Formation in the Mizunami area (Fig. 1) reported by Hayashida (1986), which are assigned to the Foraminiferal Zone N8, we reveal that significant difference of formation-mean declination is observed ($R=49.8^\circ$, $\partial R=17.2^\circ$; Fig. 8), suggesting differential rotation of the eastern part of south-west Japan since the late Early Miocene. In the Nohi area (Fig. 1), which is located between the Yatsuo and the Mizunami area, Otofuji *et al.* (1999) also suggested differential rotaion during the Miocene based on the paleomagnetic data obtained from Cretaceous to Paleogene welded tuff. In order to examine spatial difference in more various areas relative to the Yatsuo area, further investigation of precise age assignment in compared area is still necessary. In the next section, we argue temporal difference based on the sequential data obtained from the Yatsuo area for the understanding of rotational process.

4.3 Tectonic and paleoenvironmental implications

Earlier stage of rotation in the Yatsuo area is not clear because reliable paleomagnetic data were not obtained from the strata older than the Iwaine Formation. The present result, however, has confirmed that rotational process has a phase of rapid rotation in its final stage between the Iozen and Kurosedani Formations, which correspond to a period of active volcanism and subsequent period of marine transgression.

Chiji (1986) reported that paleobathymetric estimation based on benthic foraminifers in the lower Kurosedani Formation was 100-200 m, whereas the upper Kurosedani Formation and the lower Higashibessho Formation were suggested to have deposited at around 1,000-1,500 m in depth. Such remarkable change in water depth is not accommodated by global sea-level fluctuation since the Miocene (up to 200 m; Haq *et al.*, 1987), requiring tectonic subsidence linked to formation of back-arc basin. Although Hiroki and Matsumoto (1999; 2003) suggested that sequence boundaries in Miocene strata of the central Japan including the Yatsuo area were formed by regional sea-level changes using sequence stratigraphic analysis and magnetostratigraphic correlation, their interpretations should be reconsidered for two following reasons. One reason is that we refined magnetostratigraphy in the Yatsuo area. This means the correlations of sequence boundaries between the basins in central Japan by them have lost the stratigraphic basis. The other is that they underestimated the amount of the subsidence in the Yatsuo area because they ignored the result of Chiji (1986) without any reason. It seems difficult to discuss sequence boundaries from a viewpoint of global sea level changes where such large tectonic subsidence as mentioned above occurred.

Paleoenvironmental change and the paleomagnetic result of this study suggest that intensive subsidence is synchronous with the rapid rotation stage during the deposition of the Iozen and Kurosedani Formations. Japan Sea opening event might have a final phase of rapid rotation during the late Early Miocene, which seems to have caused a marine transgression in relation to remarkable subsidence in the coastal area of the Japan Sea.

5. Conclusions

1. In the Yatsuo area upon the Japan Sea coast which is underlain by the Lower to Middle Miocene, paleomagnetic measurements are conducted on samples from 26 sites and 16 sites gave primary components. Untilted paleomagnetic data combined with the previous data are composed of 10 normal and 27 reversed polarity sites of the Yatsuo Group.
2. We constrained magnetostratigraphy by the biostratigraphic data and radiometric ages. Present result suggests that the Yatsuo Group is assigned from the late Early to early Middle Miocene.
3. Significant stage of rotation as much as 30° is specified between the stage of the Iozen and Kurosedani Formations which assigned to late Early Miocene. On the basis of stratigraphic order of the back-arc opening events, this stage of rapid rotation corresponds to a period of active volcanism and subsequent period of marine transgression.
4. Japan Sea opening event might have a phase of rapid rotation in its final stage, which seems to have caused marine transgression associated with remarkable subsidence along the rifted continental margin.

Acknowledgements: We are grateful to Dr. N. Ishikawa for the use of rock-magnetic laboratory at Kyoto University. We also thank T. Miyazaki, T. Furubayashi and Y. Takiuchi for their help during the field work. Constructive reviews by Dr. H. Oda improved this manuscript.

References

Barron, J. A. and Gladenkov, A.Y. (1995) Early Miocene to Pleistocene diatom biostratigraphy of Leg 145. *In* Rea, D. K., Basov, I. A., Scholl, D. W. and Allan, J. F., eds., *Proc. Ocean Drilling Program, Sci. Results*, College Station TX (Ocean Drilling Program), **145**, 3-19.

Beck, M. E. Jr. (1980) Paleomagnetic record of plate-margin tectonic processes along the western edge of North America. *Journal of Geophysical Research*, **85**, 7115-7131.

Berggren, W. A., Kent, D. V., Swisher, C. C. III and Aubry, M. -P. (1995) A revised Cenozoic geochronology and chronostratigraphy. *SEPM Special Publication*, **54**, 129- 212.

Cande, S. C. and Kent, D. V. (1995) Revised calibration of geomagnetic polarity time scale for the Late Cretaceous and Cenozoic. *Journal of Geophysical Research*, **100**, 6093-6095.

Chiji, M. (1986) Several problems on the formation of the Japan Sea and related geological events. *Kaiyokagaku*, **18**, 188-191.

Haq, B. U., Hardenbol, J. and Vail, P. R. (1987) Chronology of fluctuating Sea levels since the Triassic. *Science*, **235**, 1156-1167.

Hayakawa, H. and Takemura, A. (1987) The Neogene System in the Yatsuo area, Toyama Prefecture, central Japan. *Journal of the Geological Society of Japan*, **93**, 717-732.

Hayashida, A. (1986) Timing of rotational motion of Southwest Japan inferred from paleomagnetism of the Setouchi Miocene Series. *Journal of Geomagnetism and Geoelectricity*, **38**, 295-310.

Hayashida, A., Fukui, T. and Torii, M. (1991) Paleomagnetism of the Early Miocene Kani Group in Southwest Japan and its implication for the opening of the Japan Sea. *Geophysical Research Letters*, **18**, 1095-1098.

Hiroki, Y. and Matsumoto, R. (1999) Magnetostratigraphic correlation of Miocene regression-and-transgression boundaries in central Honshu, Japan. *Journal of the Geological Society of Japan*, **105**, 87-107.

Hiroki, Y. and Matsumoto, R. (2003) Correlation of Miocene (18-12 Ma) sequence boundaries in central Japan to major Antarctic glaciation events. *Sedimentary Geology*, **157**, 303-315.

Ishikawa, N. (1997) Differential rotations of north Kyushu Island related to middle Miocene clockwise rotation of SW Japan. *Journal of Geophysical Research*, **102**, 17729-17745.

Itoh, Y. (1988) Differential rotation of the eastern part of southwest Japan inferred from paleomagnetism of Cretaceous and Neogene rocks. *Journal of Geophysical Research*, **93**, 3401-3411.

Itoh, Y. and Hayakawa, H. (1988) Magnetostratigraphy of Neogene rocks around the Yatsuo area in Toyama Prefecture, Japan. *Journal of the Geological Society of Japan*, **94**, 515-525.

Itoh, Y. and Hayakawa, H. (1989) On the boundary of polarity chron C5B/C5C in the Neogene section of the Yatsuo area in Toyama Prefecture, Japan. *Journal of the Geological Society of Japan*, **95**, 133-136.

Itoh, Y. and Ito, Y. (1989) Confined ductile deformation in the Japan arc inferred from paleomagnetic studies. *Tectonophysics*, **167**, 57-73.

Itoh, Y. and Kitada, K. (2003) Early Miocene rotational process in the eastern part of south-west Japan inferred from paleomagnetic studies. *The Island Arc*, **12**, 348-356.

Itoh, Y. and Watanabe, M. (2000) Refined magnetostratigraphy of the Early Miocene sequence in the Yatsuo area, central Japan. *Bulletin of the Geological Survey of Japan*, **51**, 37-45

Itoh, Y. and Watanabe, M. (2006) Fission-track dating and paleomagnetic polarity of the Lower Miocene in the Yatsuo area, central Japan. *Bulletin of the Geological Survey of Japan*, **56**, 425-429.

Itoh, Y., Yamamoto, A., Iwano, H., Danhara, T. and Watanabe, M. (2000) Paleomagnetism and fission-track ages of the Miocene sequence in the Kanazawa and Iozen areas, central Japan. *Bulletin of the Geological Survey of Japan*, **51**, 495-504.

Jolivet, L., Tamaki, K. and Fournier, M. (1994) Japan Sea, opening history and mechanism: a synthesis. *Journal of Geophysical Research*, **99**, 22237-22259.

Kirschvink, J. L. (1980) The least-squares line and plane and the analysis of palaeomagnetic data. *Geophysical Journal of the Royal Astronomical Society*, **62**, 699-718.

Lowrie, W. (1990) Identification of ferromagnetic minerals in a rock by coercivity and unblocking temperature properties. *Geophysical Research Letters*, **17**, 159-162.

McFadden, P. L. and McElhinny, M. W. (1988) The combined analysis of remagnetization circles and direct observations in palaeomagnetism. *Earth and Planetary Science Letters*, **87**, 161-172.

Nozawa, T. and Sakamoto, T. (1960) *Geology of the Yatsuo District*, with Geological Sheet Map at 1:50000. Geological Survey of Japan, Tsukuba (in Japanese with English abstract).

Otofuji, Y. and Matsuda, T. (1983) Paleomagnetic evidence for the clockwise rotation of Southwest Japan. *Earth and Planetary Science Letters*, **62**, 349-359.

Otofuji, Y. and Matsuda, T. (1984) Timing of rotational motion of Southwest Japan inferred from paleomagnetism. *Earth and Planetary Science Letters*, **70**, 373-382.

Otofuji, Y., Hayashida, A. and Torii, M. (1985) When was the Japan Sea opened ?: Paleomagnetic evidence from

Southwest Japan. *In* Nasu, N., Uyeda, S., Kushiro, I., Kobayashi, K. and Kagami, H., eds., *Formation of Active Ocean Margins* (Terra Publishing, Tokyo), 551-566.

Otofuji, Y., Itaya, T. and Matsuda, T. (1991) Rapid rotation of southwest Japan - paleomagnetism and K-Ar ages of Miocene volcanic rocks of southwest Japan. *Geophysical Journal International*, **105**, 397-405.

Otofuji, Y., Enami, R., Yokoyama, M., Kamiya, K., Kuma, S., Saito, H. and Matsuda, T. (1999) Miocene clockwise rotation of southwest Japan and formation of curvature of the Median Tectonic Line: Paleomagnetic implications. *Journal of Geophysical Research*, **104**, 12895-12907.

Shibata, K. (1973) K-Ar ages of volcanic rocks from the Hokuriku Group. *The Memoirs of the Geological Society of Japan*, **8**, 143-149.

Tamaki, K. (1986) Age estimation of the Japan Sea on the basis of stratigraphy, basement depth, and heat flow data. *Journal of Geomagnetism and Geoelectricity*, **38**, 427-446.

Watanabe, M. and Yanagisawa, Y. (2005) Refined early to middle Miocene diatom biochronology for the middle- to high-latitude North Pacific. *The Island Arc*, **14**, 91-101.

Yanagisawa, Y. (1999a) Diatom biostratigraphy of the Miocene sequence in the southern Kanazawa area, Ishikawa Prefecture, central Japan. *Bulletin of the Geological Survey of Japan*, **50**, 49-65.

Yanagisawa, Y. (1999b) Diatom biostratigraphy of the lower to middle Miocene sequence in the Yatsuo area, Toyama Prefecture, central Japan. *Bulletin of the Geological Survey of Japan*, **50**, 139-165.

Received January 10, 2006
Accepted August 29, 2006

富山県八尾地域に分布する下部－中部中新統の古地磁気学的研究

玉置真知子, 伊藤康人, 渡辺真人

要　旨

新第三紀における日本海拡大イベントに関連した回転運動プロセスを調べるため，富山県八尾地域に分布する下部 - 中部中新統の八尾層群にて古地磁気学的研究を行った．調査地域における山田川ルート，和田川ルートで得られた火山岩，堆積岩から段階消磁実験を行った結果，16地点の安定した初生磁化成分が分離できた．これまでに八尾地域で報告されている全37地点の古地磁気データを統括すると，傾動補正後の地点平均方位において，正帯磁を示すものが10地点，逆帯磁を示すものが27地点得られた．回転運動の経過を詳細に知るために，各層準に対する偏角の推移を調べた結果，経時変化が見られ，時計回りの回転運動の記録が捉えられていることが明らかになった．累層ごとに分けた平均方位の偏角の比較では，医王山層と黒瀬谷層の間で約30度の有意差を示す．本論で確立した古地磁気層序に基づくと，医王山層と黒瀬谷層は前期中新世末期に対比される．また，古地磁気方位と岩相変化を比較すると，急激な回転運動は火成活動の盛んな時期から海進に伴う堆積物供給期間の転換期にあたる．日本海拡大イベントには，その後半に急激な回転運動のフェーズが存在し，その結果，本研究地域である日本海沿岸の堆積盆に顕著な環境変化をもたらした可能性がある．